Material Science Research India Vol. **5**(1), 49-58 (2008)

Voltammetric studies of the onset of NAAAS micellizations and its corrosion inhibition for carbon steel

SHALABY A. YASIN*

Chemistry Department, Faculty of Science, Benha University, Benha (Egypt)

(Received: January 23, 2008; Accepted: May 11, 2008)

ABSTRACT

The critical micelle concentration (CMC) as well as the diffusion coefficients of the synthesized NaAAS surfactant were determined and discussed. The voltammetry of probed ferrocene solubilized in NaAAS surfactant was investigated using three different electrochemical techniques such as cyclic voltammetry, rotating disk voltammetry and chronocoulometry from aqueous buffer carbonate solutions of pH 10. The CMC of NaAAS was found to be 4.0×10^{-4} M using both CV and RDV techniques. Chronocoulometry showed negligible adsorption contribution to the electrode surface (1.0×10^{-15} M). The apparent diffusion coefficients were estimated from RDV measurements and the real micelles diffusion coefficients were obtained. Reequilibrium considerations of ferrocene probe kinetics at the electrode surface was treated according to two different modes of slow- and fast-kinetics. The corrected diffusion coefficient values showed constancy at $(4.69\pm 0.4)\times10^{-7}$ cm^2/sec in the concentration range from 20 to 200 mM NaAAS. The morphological features of NaAAS micelles showed globular self-assembled structure with no conversion to rod-like at higher NaAAS concentrations. The inhibition efficiency of carbon steel L52 was determined from 1 M HCl containing different NaAAS concentrations using weight loss measurements. The maximum inhibition efficiency was obtained at 4×10^{-4} M NaAAS corresponding to the predetermined CMC of the surfactant.

Key words: Voltammetry, micelles, reequilibrium kinetics and weight loss.

INTRODUCTION

Micelles are dynamic aggregates of amphiphilic or surfactant molecules possessing both hydrophilic and hydrophobic character[1]. In such systems, both oil.soluble and water.soluble compounds can be dissolved due to the simultaneous presence of aqueous and non.aqueous domains. Since the reagents are localized in either aqueous or nonaqueous domain at the pseudophase, their effective local concentrations are increased. This can increase reaction rates[2-4]. Electrochemical techniques have been applied as tool for the characterization of micelles and microemulsion systems[5.9].

In general voltammetry in microheterogeneous systems, such as micelles[10], microemulsions[11] and macroemulsions[12] is becoming increasingly popular as a general method for studying heterogeneous redox processes and for characterizing the discontinuous phase in such systems. These systems have important industrial[13-16] and biomedical applications[17-19] and warrant a thorough understanding of many subjects such as the related transport phenomena, structure of the pseudophase, electrode processes and many others. The micelles particle size is determined from the estimated diffusion coefficients using the Stokes.Einstein equation[20].

$$D = \frac{KT}{6\pi\eta r_h}$$

where K is the Boltzmann constant, T is the absolute temperature, h is the viscosity coefficient and r_h is the hydrodynamic radius of the droplet. Generally, electrochemical (EC) techniques probed self-diffusion coefficients compared to

quasi.elastic light scattering (QELS) technique and showed good agreement with those obtained from NMR because they possess very long diffusion time (~ 1 msec). Therefore, both EC and NMR techniques probe self.diffusion over a distance larger than the extension of any aggregate in solution. Whereas, in QELS measurements it showed collective data and the time scale is very short in the range of 0.1 to 10 msec.

This paper is devoted for the voltammetric detection of the onset of micellization and diffusion coefficient determinations of the synthesized, NaAAS surfactant using three different electrochemical techniques such as CV, RDV and CC. Reequilibrium kinetic considerations of ferrocene probe partitioning and solubilization studies are discussed. The protection of carbon steel L52 using NaAAS surfactant was measured by weight loss measurements.

EXPERIMENTAL

Material

Acrylonitrile, acrylic acid, oleic acid were obtained from Aldrich. Ferrocene, NaCl, HCl and NaOH were certified ACS reagents.

Acrylamidostearic acid (AAS) was prepared by reacting acrylonitrile and oleic acid according to the method of Greene[21]. The crude material was then dissolved in absolute ethanol and after filtering any insoluble residue, it is neutralized with sodium ethoxide. The addition of dry acetone to the neutralized ethanolic solution of acrylamidostearic acid, AAS, precipitates sodium acrylamidostearate (NaAAS). After repeatedly washing with dry acetone, it was then dried under vacuum at room temperature overnight. The recrystallized material was identified using FTIR, absorption bands appeared at 3080, 1620, 980 and 945 cm^{-1} corresponding to the terminal vinyl group (CH_2 = CH-) while 3260, 1650 and 1560 cm^{-1} absorption bands were corresponded to the absorptions of amide group (-CONH-). Therefore the structural formula will be as shown below:

$$CH_3(CG_2)_{8(7)}\text{-}CH(CH_2)_{8(7)}\text{-}COONa$$
$$|$$
$$NHCOCH = CH_2$$
(NaAAS)

Table 1: Electrochemical data obtained for 0.07 mM ferrocene in 1 mM NaAAS surfactant using cyclic voltammetry at 25°C

Scan Rate mV/sec	i_{pc} µA	i_{pa} µA	E_{pc} µV	E_{pa} µV	i_{pa}/i_{pc} -	ΔE_p mV
20	0.658	0.695				
40	0.774	0.820				
60	1.368	1.316				
80	1.620	1.580				
100	1.895	1.789				
150	2.350	2.268				
200	2.902	2.870				

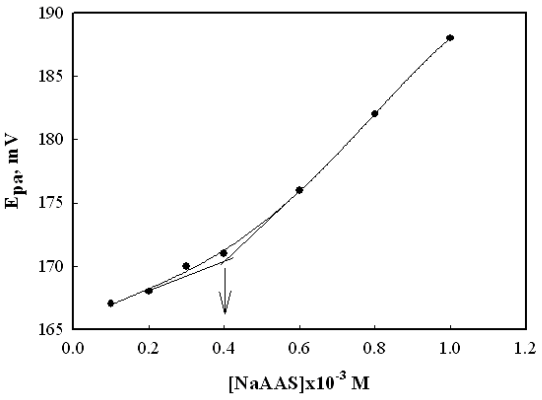

Fig. (1): The plot of anodic peak potentials of ferrocene at different NaAAS concentrations

[NaAAS] x 10^{-3}

Fig. 1: The plot of anodic peak potential of ferrocene at different NaAAS concentrations

Equipment

The electrochemical measurements such as cyclic voltammetry (CV), rotating disk voltammetry (RDV) and chronocoulometry (CC) were conducted using Electrochemical Analyser Model HQ-2030 and the rotating disk electrode from BAS. A three compartment cell consisted of glassy carbon as working electrode, platinum foil (1 cm^2) as counter electrode and saturated calomel electrode (SCE) as the reference electrode used in electrochemical measurements.

The glassy carbon electrode was cleaned up by successive polishing with 0.3 and down to 0.05 mm sized alumina and thoroughly washed with distilled water, finally ultrasonicated in distilled water for 15 minutes to dislodge the retained aluminum oxide particles from the electrode surface. The area of the glassy carbon (GC) electrodes used for both cyclic voltammetry (CV) and rotating disk voltammetry (RDV) were estimated using cyclic voltammetry techchnique from 4 mM $K_4[Fe(CN)_6]$ dissolved in 1 M KCl solution of known diffusion coefficient ($D = 6.32 \times 10^{-6}$ cm^2/sec) [22]. It was found to be 0.067 and 0.453 cm^2 for both techniques; respectively. In electrochemical measurements, the surfactant solutions were deaerated by bubbling a stream of nitrogen gas for at least 10 min using slow rate to avoid foaming.

Spectral measurements were conducted using Perkin.Elmer spectrophotometer Model Jasco V-500. All electrochemical measurements were recorded for the first scan and recorded at 25°C using HAAke water circulator bath.

Table 2: Electrochemical data obtained from rotating disk voltammetry around the critical micelle concentration of NaAAS surfactant containing 0.1 M NaCl at pH 10.0, using fixed 0.07 mM of ferrocene, 25°C

[NaAAS] mM	$\Delta i_l/\omega\Delta^{1/2}$ μA.sec	S/S_0 -	D_a (cm^2/sec)
0.00(*)	1.047	1.000	6.70×10^{-6}(*)
0.10	1.042	0.995	4.00×10^{-6}
0.20	1.010	0.965	3.82×10^{-6}
0.30	0.960	0.917	3.54×10^{-6}
0.40	0.748	0.715	2.44×10^{-6}
0.80	0.638	0.610	1.92×10^{-6}
1.00	0.618	0.590	1.83×10^{-6}
2.00	0.565	0.540	1.60×10^{-6}
4.00	0.502	0.480	1.34×10^{-6}
8.00	0.450	0.430	1.14×10^{-6}
10.00	0.441	0.422	1.10×10^{-6}

*Ref. 18.

Table 3: Apparent diffusion coefficients and its treatment according to slow- and fast-kinetic limits obtained for NaAAS surfactant using rotating disk voltammetry at 25°C

[NaAAS] mM	[Fc] mM	D_a cm^2/sec	$D_d^{(a)}$ cm^2/sec	$D_d^{(b)}$ cm^2/sec
20	0.30	6.40×10^{-7}	7.69×10^{-7}	-
40	0.55	6.30×10^{-7}	3.06×10^{-7}	2.30×10^{-8}
60	0.81	6.21×10^{-7}	3.99×10^{-7}	2.20×10^{-7}
80	0.98	6.10×10^{-7}	5.68×10^{-7}	2.83×10^{-7}
100	1.25	5.90×10^{-7}	4.47×10^{-7}	3.35×10^{-7}
150	1.50	5.90×10^{-7}	4.71×10^{-7}	3.79×10^{-7}
200	2.00	5.80×10^{-7}	4.91×10^{-7}	4.20×10^{-7}

a- slow-kinetic treatment

b-fast-kinetic treatment

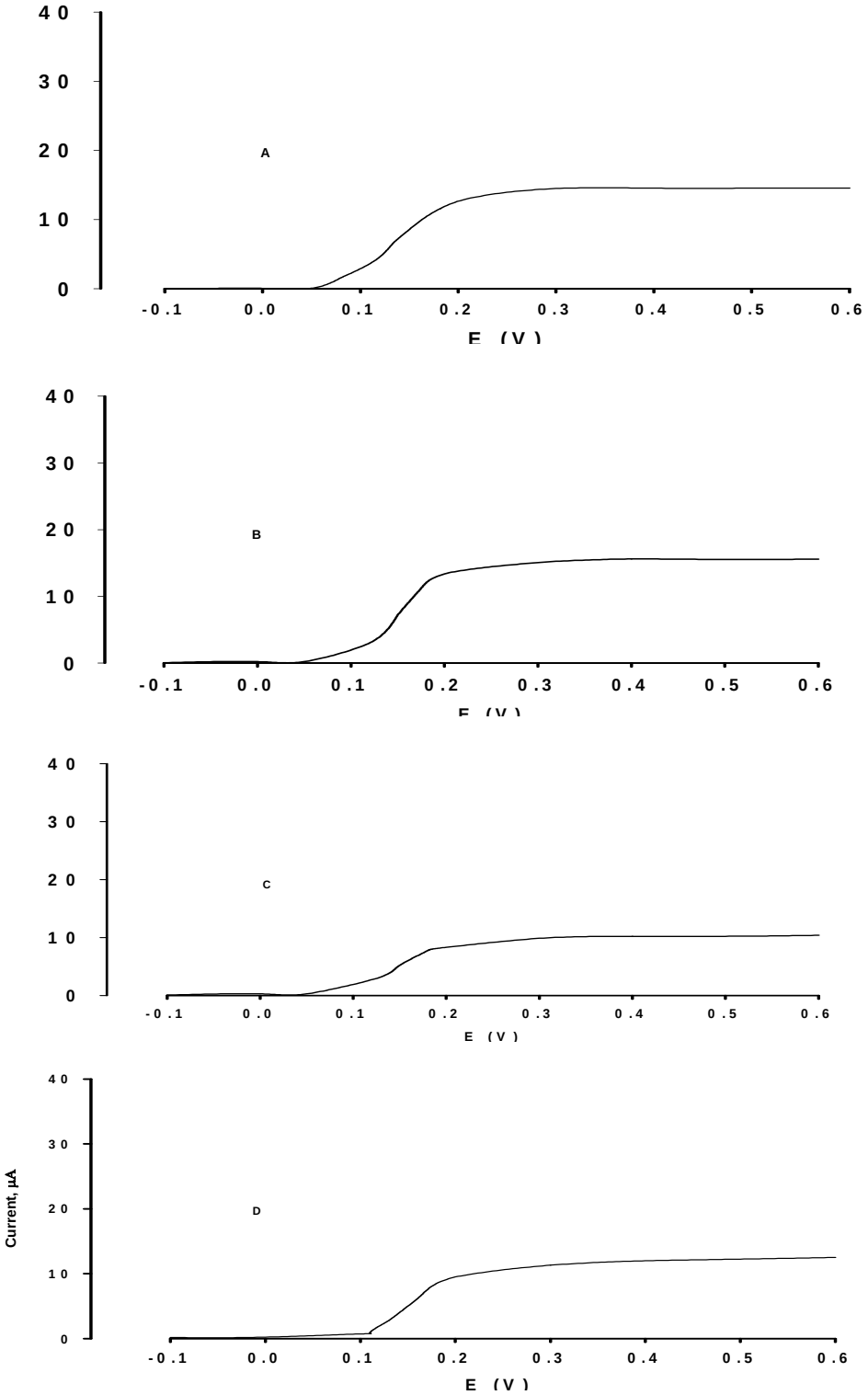

Fig. 2: RDV voltammograms recorded at 1000 RPM for: A- 4x10^{-4} M, B- 8x10^{-4}, C-2×10^{-4} M and D-8×10^{-3} M NaAAS

Table 4: The effect of anionic NaAAS concentrations on the weight loss measurements of carbon steel L52 corrosion in 1.0 M HCl

[NaAAS] ppm	M	Weight Loss (mg/d.cm^2)	Inhibition efficiency (IE%)
15.0	4.0×10^{-5}	200.0	64.28
30.0	8.0×10^{-5}	180.0	67.86
37.5	1.0×10^{-4}	170.0	69.64
75.0	2.0×10^{-4}	140.0	75.00
150.0	4.0×10^{-4}	42.0	92.50
225.0	6.0×10^{-4}	42.0	92.50
300.0	8.0×10^{-4}	41.0	92.68
375.0	1.0×10^{-3}	41.2	92.64

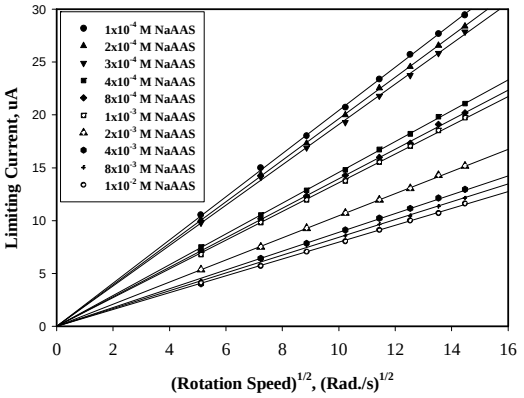

Fig. 3: The plots of limiting current of 7×10^{-5} M ferrocene in different [NaAAS] at different rotation speeds

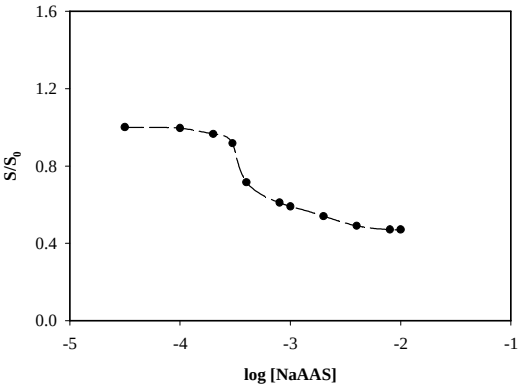

Fig. 4: The plots of the slope ratio (S/So) at different surfactant concentrations

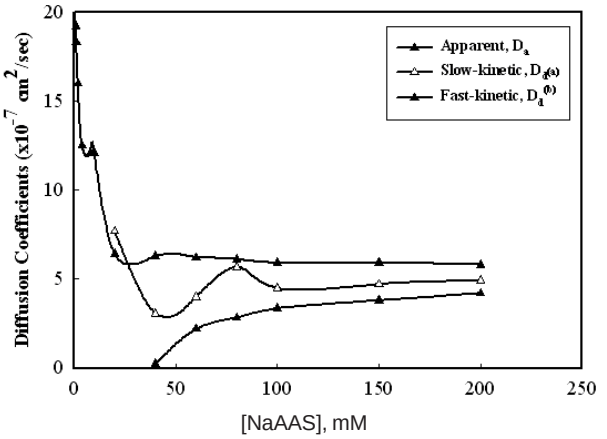

Fig. 5: The plots of the apparent diffusion coefficient and its corrections by slow and fast-methods at different [NaAAS]

Carbon steel sheets with dimensions of 1×2×0.2 cm were used in the weight loss measurements. A stock solution of 1×10^{-2} M NaAAS was prepared in absolute ethanol from Merk for the weight loss measurements. Each carbon steel sheet was immersed for six hours in 1M HCl solutions containing different NaAAS concentrations and recorded in quartet replicates.

RESULTS AND DISCUSSION

Determination of the onset of micellization

Cyclic voltammetry (CV)

The cyclic voltammograms of fixed ferrocene (Fc) concentration (7.0×10^{-5} M) solubilized in sodium acrylamidostearate (NaAAS) surfactant of different concentrations varied from $1.0x10^{-4}$ to $1.0x10^{-2}$ M were recorded in aqueous buffer solutions of pH 10.

The amount of ferrocene probe solubilized at the lower NaAAS concentration ($1.0x10^{-4}$ M) containing 0.10 M NaCl as supporting electrolyte of pH 10 was measured from UV.Visible spectrophotometry. Standard solutions of ferrocene were prepared in ethanol.water mixtures and measured against water as blank. By appropriate dilutions it showed absorbance 0.30 at 250 nm wavelength and had a molar absorptivity $e/10^4$ $M^{-1}.cm^{-1}$ which was found in a good agreement with that reported for CTAB[23]. The amount of ferrocene was solubilized in $1.0x10^{-4}$ M NaAAS containing 0.10 M NaCl was performed by ultrasonication for at least seven hours. Solubilizations were performed three times and the amount of ferrocene dissolved in $1x10^{-4}$ M NaAAS was measured at 250 nm using the molar absorptivity given above from the standard graph and found to be $7.0x10^{-5}$ M. Therefore, the amount of ferrocene used in subsequent electrochemical measurements and CMC determinations was fixed at this concentration level to avoid the fluctuations in peak current and diffusion coefficient values as well as having a better estimate.

The voltammograms recorded at different scan rates from 20.500 mV/sec showed a single redox peak. Ferrocene is well behaved reversibly in these media at different surfactant concentrations. The peak potential separation ΔE_p (= E_{pa} - E_{pc}) is always kept in the range of 55.59 mV and the ratio of i_{pa}/i_{pc} did not exceed 1.10, Table (1). This behavior indicate the complete reversibility of ferrocene oxidations in these media with a net transfer of one electron forming ferrocenium ion (Fc^+).

The peak current of reversible system is described by the Randles. Sevcik equation [24] for the forward step of the first cycle, plot

$$i_p = 0.4463nFAC_o (nF/RT)^{1/2}D_a^{1/2}\upsilon^{1/2} \quad ...(1)$$

The plots of i_{pa} versus $\upsilon^{1/2}$ showed linear correlations passing through the origin at different NaAAS concentrations indicating the diffusion nature of the electrode process[25]. The critical micelle concentration CMC is determined by observing the variation of anodic peak current for ferrocene oxidations against surfactant concentrations. The plots of i_{pa} obtained at 100 mV/sec versus [NaAAS] is linear and showed a break at $4.0x10^{-4}$ M indicating that physical and chemical changes taking place[26] by the formation of micelles. Also, the plotting of $E_{1/2}$ vs. [NaAAS] showed linear relationship consisting of two segments and the breaks occurs at $4.0x10^{-4}$ M which is further confirmed the obtained value of CMC, Fig. 1.

RDV experiments

The voltammograms of ferrocene solubilized in different concentrations of sodium acrylamidostearate (NaAAS) were recorded at different rotation speeds (ω) from 250 to 2000 RPM. The potential was scanned from -100 to 600 mV at scan rate 5 mV/sec. The rotating disk voltammograms were treated using the most practical form of completely treated rigorous hydrodynamic equation of Levich who first solved the mass transport equations of the rotating disk electrode[27]. The limiting current of a reaction controlled only by mass transfer has given by the Levich equation:

$$i_L = 0.62nFAD^{2/3}\nu^{-1/6}\omega^{1/2}C_o \quad ...(2)$$

where i_L is the limiting current (A), ν is the kinematic viscosity (cm^2/sec) and ω is the angular velocity (rad/sec). In this case ferrocene was used as the hydrophobic probe which has a solubility in aqueous solution of $5x10^{-5}$ M [5]. Therefore, accurate

measurements fulfilled by making corrections for the contribution to the electrode surface by the amount of probe solubilized in aqueous continuous phase. The Levich equation may be rewritten in the pseudophase approximation as following:

$$i_L = 0.62nFA\{D_o^{2/3}(C_o - C_m) + D_m^{2/3}C_m\}\nu^{-1/6}\omega^{1/2} \quad ...(3)$$

where C_o and D_o are the total concentration of ferrocene and aqueous phase diffusion coefficient; respectively. C_m is the concentration of ferrocene solubilized micelles and D_m is the micelle diffusion coefficient. For very dilute aqueous solutions the slope was extracted from equation (2) as following:

$$S_o = \partial i_I / \partial \omega^{½} = i_I / \omega^{½} \quad ...(4)$$

The analogous quantity derived from equation (3) divided by equation (4) it gives:

$$\frac{S}{S_o} = \left\{ \frac{C_o - C_m}{C_o} + \frac{D_m^{2/3} - C_m}{D_o^{2/3} C_o} \right\} x \frac{\nu}{\nu_o}^{-1/6} \quad ...(5)$$

The onset of micellization of NaAAS surfactant was detected from aqueous solutions of pH 10.0 containing 0.1 M NaCl at 25°C using RDV technique. The electroactive probe used was ferrocene and the surfactant concentration was varied from $1x10^{-4}$ to 0.01 M, Fig. 2. The results showed excellent linearity of i_L versus $\omega^{1/2}$ passing through the origin indicating that ferrocene is well behaved and the electrode process is under mass transfer control within the surfactant concentration range, Fig. 3.

The plots of the slope ratio (S/S_o) versus surfactant concentration, log [Surf] at 0.07 mM concentration of ferrocene showed dissociation curve as represented in Fig. 4. The critical micelle concentration was determined from the intersect of the two portions and found to be at $4×10^{-4}$ M. The slope ratio (S/S_o) was used for obtaining more accurate results avoiding fluctuation in electroactive probe concentration.

Chronocoulometry (CC)

An important aspect to be considered in electrochemical investigations in surfactant solutions is its adsorption on the electrode surface. Double potential step chronocoulometry (CC) is the most useful technique in determining the amount of adsorption of electroactive species[28,29]. In absence of product adsorption the difference of intercepts of Q versus $t^{1/2}$ and Q_r versus θ plots for both the forward and reverse reactions respectively, gives a direct measurement of the adsorbed species[30]. The amount of ferrocene probe adsorbed in NaAAS micelles was evaluated and found to be $1.0×10^{-15}$ M which considered a negligible amount as compared with the amount of probe being added ($7.0×10^{-5}$ M). This is found to be in good agreement with the results obtained from both CV and RDV experiments.

Solubilizations studies and diffusion coefficients using RDV

Diffusion coefficients

From the electrochemical oxidation of ferrocene, the plots of i_l versus $\omega^{1/2}$ at different NaAAS concentrations in the range from 20 to 200 mM) showed linear correlations passing through the origin. The concentration of ferrocene used at different surfactant concentrations were very close to the saturation concentration in each micellar solutions. Also, the amount of ferrocene solubilized in NaAAS micelles were determined spectrophotometrically as described above and listed in Table 3. The RDV voltammograms of saturated solution of ferrocene solubilized in different NaAAS concentrations were recorded at scan rate of 5 mV/sec and different rotation speeds. The plots of i_l versus $\omega^{1/2}$ using were found to be linear and passing through the origin indicating that the electrode reaction taking place under mass transfer control, Fig. 3. The apparent diffusion coefficients (D_a) were determined from the Levich eq. (2) using the slopes of the plots of i_L-$\omega^{1/2}$ plots, Table 3.

Reequilibrium and kinetic considerations from RDV

The apparent diffusion coefficient (D_a) values obtained according to the above equation is an average value, because the electroactive ferrocene has a solubility of $5x10^{-5}$ M in aqueous solution[5]. Therefore, the apparent diffusion

coefficient (D_a) obtained directly from the Levich plot is higher than actual value of micelles. The approximations that applied to diffusion coefficient determinations is termed as zero.kinetics limit[31,32] in which the reequilibrium consideration in concentration gradients at the electrode surfaces is ignored and it is thus treated additively as a parallel processes. Since, there is a static and dynamic effects of probe partitioning in micellar pseudophase, the entrance-exit kinetics of electroactive probe partitioning should be taken into account using the respective mole fractions of ferrocene in each of the aqueous and nonaqueous domains at the pseudophase. Two different modes [33] were assumed for this kind of treatments slow. and fast.kinetic considerations. Firstly, the determination of slow.kinetics consideration in which there is reequilibrium in the diffusion layer of ferrocene between pseudophases. Reequilibrium at the electrode surface is assumed to be slower than the lifetime of the current measurement. The corrected diffusion coefficient of micelles in this case is then obtained according to the following relationship[33].

$$D_d^{2/3} = D_a^{2/3}\frac{\bar{C}}{C_d} - D_c^{2/3}\frac{\bar{C}c}{C_d} \quad ...(6)$$

where C, C_d and C_c are the total (volume) concentration of ferrocene, the concentration in the micellar pseudophase and its aqueous (continuous) ferrocene concentration, respectively. D_a, D_d and D_c are the apparent diffusion coefficient, micelles diffusion coefficient and aqueous continuous diffusion coefficients, respectively.

The second mode is the fast.kinetic treatment, in which it is assumed that the reequilibrium at the pseudophase takes place faster than the lifetime of the current measurement. The diffusion coefficient corrected according to this assumption has given as following[33]:

$$D_d = D_a\frac{\bar{C} - D_c\bar{C}c}{C_d - C_d} \quad ...(7)$$

the significance of these values is previously described.

The apparent diffusion coefficient values (D_a) obtained electrochemically from RDV and its corrected values (D_d) according to the above equations (6) and (7) were plotted versus NaAAS concentrations, Fig. 5. Inspection of the diffusion coefficient values obtained by slow- and fast- kinetic corrections showed constancy of the diffusion coefficient values on increasing NaAAS concentrations at about (4.69 ± 0.4) $x10^{-7}$ cm^2/sec. The micellar sizes were determined by substituting in Stokes.Einstein equation described above after correcting the viscosity coefficient showing constancy at about 58 ^oA diameter. This behavior indicates that globular self.assembly structure rather than rod.like takes place at higher NaAAS concentration. Since the size of NaAAS does not practically changes, the number of micelles increases yielding more repulsive interactions as reported for SDS[34] and CTAB[35] and others.

NaAAS Surfactant as Corrosion Inhibitor

Due to the various industrial applications and economic importance of carbon steel, its protection against corrosion has attracted much attention. The carbon steel (L-52) sheets used in this study had the following composition on the basis of weight percentages; 0.26 C, 1.35 Mn, 0.04 P, 0.05 P, 0.05 S, 0.005 Nb, 0.02 V, 0.03 Ti and the remainder is iron. The use of inhibitors is one of the most practical methods for protection[36,37]. Surfactant compounds were tested as corrosion inhibitors for carbon steel and found to have high inhibition efficiencies[38-41]. Since some corrosion inhibitors used at lower concentrations may accelerate corrosion or causes emulsification at higher concentrations it is necessary to study the effect of surfactant concentration on the inhibition efficiency (IE) and its relation to micelles formations using weight loss measurements.

The loss in the weight of carbon steel sheets due to their immersion in 1 M HCl solutions containing different concentrations of anionic NaAAS surfactant was measured. It was found that the addition of NaAAS surfactant at any concentration level lowers the weight loss of carbon steel than its value in the corrosive medium. This result indicates that NaAAS acts as inhibitor for carbon steel in the presence of aggressive anions. The inhibitive effect could be attributed to the

adsorption of surfactant molecules on carbon steel forming a barrier between the bar metal and the corrosive medium[37]. The surface activity of NaAAS and its adsorption is facilitated by the presence of the carbonyl of the amide. group in its structure as well as the unsaturation center. The adsorbed surfactant molecules onto metal surface is oriented via the hydrophilic amido. group whereas the hydrocarbon domains is oriented toward the aqueous solution. Since the hydrocarbon chain is hydrophobic in its nature it repels the aqueous aggressive anions away from the metal surface and therefore inhibit the corrosion process. The inhibition efficiencies (IE%) of carbon steel strips immersed for 6 hours in 1M HCl solutions in absence and presence of different NaAAS concentrations was determined and given in Table (4). The inhibition efficiency (IE) is determined according to the following equation [36]:

$$IE\% = [(W_f - W_i)/ W_f] \times 100$$

where W_f and W_i are the weight loss of strips in the free and inhibited acidic solutions, respectively. Inspection of the values of weight loss measurements revealed that as the surfactant concentration increases as the weight loss decreased till reaching certain concentration at which the maximum efficiency was obtained. 4×10^{-4} M (150 ppm) NaAAS displayed the maximum inhibition efficiency. This concentration is corresponding to the CMC of the anionic surfactant which is determined above electrochemically using both cyclic voltammetry and rotating disk voltammetry. At this concentration level the simple surfactant molecules changed to aggregates (spherical micelles) of particle size 58°A. Above the CMC the inhibition efficiency reached to almost constant value. This behavior is attributed to the constancy of micelles particle size where the morphological features of NaAAS micelles showed spherical drops with no conversion to rod like ones. Therefore, the inhibition efficiency increases via preferential adsorption of the highly negatively charged hydrophilic domains of the associated micelles via the amido-group while the hydrocarbon domains protude brush-like into solution.

REFERENCES

1. Fendler J.H., Fendler E.J. "*Catalysis in Micellar and Macromolecular Systems*", Academic Press, New York, (1975).
2. Pelizzetti, E., Pramauro E., J. *Anal. Chim. Acta*, **1**: 169 (1985).
3. Burgess J., *Colloids Surf*., **48**: 185 (1990).
4. Minero C., Pramauro E., Pelizzetti E., *Colloids Surf*., **35**: 237(1989).
5. Georges J., Demettre S., *Electrochimica Acta*., **29**: 521(1984); **31**: 1519(1986).
6. Mahajan R.K., Kaur N. and Bakshi M.S., *Colloids Surf.,* **225**: 33 (2005).
7. Zana R. and Mackay R.A., *Langmuir*, **2**: 109 (1986).
8. Shipovskov S., Ferapotova E., Ruzgas T. and Levashov A., *Biochimica et Biophysica Acta,* (2003).
9. Lu X., Zhang M., Kang J., Wang X., Zhuo L. and Liu H., *J. Inorg. Biochem.,* (2004).
10. Matsubara T. and Texter J., *J. Colloid Interface Sci.* **112**: 42 (1986).
11. Georges J. and Desmettre S., *J. Dispersion Sci. Technol.* **7**: 21 (1986).
12. Texter J., Beverly T., Templar S. R. and Matsubara T., *J. Colloid Interface Sci.* **120**: 389 (1987).
13. Morishita M., Shimizu Y., Kobayakawa K. and Sato Y., *Electrochimica Acta*, **53**(22): 6651 (2008).
14. Shinoda K., Ed., *Solvent Properties of Surfactant Solutions*, Marcel Dekker, New York, Vol. **2** (1967).
15. Shah D. O., Ed., *Macro and Microemulsions*: *Theory and Applications*, Am. Chem. Soc. Symposium Ser., Washington D.C., 272 (1985).

16. Shah D. O. and Schecter R. S., Eds., *Improved Oil Recovery by Surfactant and Polymer Flooding*, cademic Press, New York (1977).
17. Spieser P. In *Reverse Micelles*, Luisi P. L., Straub B. E., Eds., Plenum, New York (1984).
18. Mackay R. A., *Adv. Colloid Interface Sci*. **15**, 131 (1981).
19. Lichtenberg D., Robson R. J. and Dennis E. A., *Biochim. Biophys. Acta* **737**: 285 (1983).
20. Einstein A., *Ann. Phys.,* **19**, 289 (1906).
21. Greene B.W., Sheetz D.P. and Filler T.D., *J. Colloid Interface Sci.,* **32**: 90 (1970).
22. Von Stackelberg M., Pilgram M. and Toome V., *Z. Electrochem.,* **57**: 342 (1953).
23. Ohsawa Y. and Aoyagui S., *J. Electroanal. Chem*. **136**: 353 (1982).
24. Adams A. J., "*Electrochemistry at Solid Electrodes*" Dekker (1969).
25. Bard A. J. & Faulkner L. R., "*Electrochemical Methods Fundamentals and Applications*", John Wiley, New York, 218 (1980).
26. Mandal A. B., Nair B. U. and Ramaswamy D., *Langmuir* **4**: 736 (1988).
27. Levich V.G., *Acta Phyhsicochim. USSR* **17**: 157 (1942).
28. Anson F.C., *Anal. Chem*. **38**, 54 (1966).
29. Turner J.A., Turner B.A. and Darkinson B.A., *J. Electroanal. Chem*. **150**: 611 (1983).
30. Anson F.C. and Osteryoung R.A., *J. Chem. Educ*. **60**: 293 (1983).
31. Dayalan E., Qutubuddin S. and Texter J., *J. Colloid Interface Sci*. **143**: 423 (1991).
32. Texter J., *J. Electroanal. Chem*. **304**: 257 (1991).
33. Dayalan E., Qutubuddin S. and Texter J., *J. Colloid Interface Sci*. **158**: 249 (1993).
34. Corti M. and Degiorgio V., *J. Phys. Chem*. **85**, 711 (1981).
35. Dorshow R. B., Briggs J., Bunton C.A. and Nicoli D. F., *J. Phys. Chem*. **86**: 2388 (1982).
36. Mathur P.B. and Vasudevan T., *Corrosion,* **38**: 17 (1982).
37. Tedeschi R.J., *Corrosion,* **31**: 130 (1975).
38. Keera S.T.: *Br. Corros. J.,* **36**(4): 26 (2001)
39. Osman M.M.: *Anti.Corros. Methods and Materials,* **45**(3): 176 (1998).
40. Al Sobagh A.M., Osman M.M., Omar A.A. and El.Gamal I.M.: *Anti.Corros. Methods and Materials,* **43**: 11 (1996).
41. Al Amrousiz F.A., Al Sobagh A.M. and Osman M.M.: *Fuel,* **75**: 1193 (1996).